Title: Meiotic drive of female-inherited supernumerary chromosomes in a pathogenic fungus

Authors: Michael Habig[1], Gert H.J. Kema[2] and Eva H. Stukenbrock[1*]

Author affiliation:

1) Environmental Genomics, Christian-Albrechts University of Kiel, Kiel, and the Max Planck Institute for Evolutionary Biology, Plön, Germany,

2) Wageningen Plant Research, Wageningen University and Research, and Laboratory of Phytopathology, Wageningen University and Research, Wageningen, The Netherlands

*Corresponding Author:

Eva H. Stukenbrock

Am Botanischen Garten 11

24118 Kiel, Germany

Tel: +49 431 8806368

email: estukenbrock@bot.uni-kiel.de

Abstract

Meiosis is a key cellular process of sexual reproduction involving the pairing of homologous sequences. In many species however, meiosis can also involve the segregation of supernumerary chromosomes, which can lack a homolog. How these unpaired chromosomes undergo meiosis is largely unknown. In this study we investigated chromosome segregation during meiosis in the haploid fungus *Zymoseptoria tritici* that possesses a large complement of supernumerary chromosomes. We used isogenic whole chromosome deletion strains to compare meiotic transmission of chromosomes when paired and unpaired. Unpaired chromosomes inherited from the male parent as well as paired supernumerary chromosomes showed Mendelian inheritance. In contrast, unpaired chromosomes inherited from the female parent showed non-Mendelian inheritance but were amplified and transmitted to all meiotic products. We concluded that the supernumerary chromosomes of *Z. tritici* show a meiotic drive and propose an additional feedback mechanism during meiosis which initiates amplification of unpaired female-inherited chromosomes.

In eukaryotes meiosis is a highly conserved mechanism that generates gametes and facilitates recombination by pairing of homologous chromosomes. Meiosis combines one round of DNA replication with two subsequent rounds of chromosome segregation (reviewed in (*Klutstein and Cooper, 2014; Zickler and Kleckner, 2015*)). DNA replication during the meiotic S-phase progression is coupled directly to interactions between homologous sequences and results in the pairing of chromosomes and recombination (*Cha et al., 2000*). The initial pairing of homologous chromosomes is important for meiosis and proper chromosome segregation (reviewed in (*Loidl, 2016*)). However, it is less clear how meiosis proceeds when pairing of homologous chromosomes does not take place due to unequal sets of chromosomes, as is the case in organisms with non-essential supernumerary chromosomes.

Supernumerary chromosomes, also known as B chromosomes, conditionally dispensable chromosomes or accessory chromosomes, are present in some but not all members of a population, and estimated to be present in 14% of karyotyped orthopteran insect species (*Jones, 1995*), 8% of monocots, and 3% of eudicot species (*Levin et al., 2005*). These chromosomes commonly show non-Mendelian modes of inheritance, leading to segregation distortion during meiosis and a change in the frequency of the supernumerary chromosome in the progeny – a process that has been described as a chromosome drive (*Jones et al., 2008; Valente et al., 2017*). Segregation advantage of supernumerary chromosomes can be due to drive mechanisms at the pre-meiotic, meiotic, or post-meiotic stages of gamete formation (*Hasegawa, 1934; Houben et al., 2014; Houben, 2017; Mroczek et al., 2006; Ohta, 1996*) and has been demonstrated in animals and plants (*Akera et al., 2017; Mroczek et al., 2006*). In fungi, supernumerary chromosomes have been characterized in several species and notably studied in fungal pathogens where their presence in some cases is associated with virulence (*Ma et al., 2010; Miao et al., 1991*). The underlying mechanisms causing non-Mendelian inheritance of the supernumerary chromosomes in fungi are however poorly understood.

The genomic composition of the fungal plant pathogen *Zymoseptoria tritici* provides an attractive model to analyze supernumerary chromosome transmission. The genome of this fungus contains one of the largest complements of supernumerary chromosomes reported to date (*Goodwin et al., 2011*). The eight distinct supernumerary chromosomes (chr14 to chr21) of the reference isolate IPO323 show presence/absence polymorphisms among isolates and differ in their genetic composition compared to the essential chromosomes (*Goodwin et al., 2011; Plissonneau et al., 2016*). The supernumerary chromosomes in *Z. tritici* are enriched in repetitive elements (*Dhillon et al., 2014; Goodwin et al., 2011; Grandaubert et al., 2015*), mainly heterochromatic (*Schotanus et al., 2015*) and frequently lost during mitosis (*Moeller et al., 2018*) and meiosis (*Croll et al., 2013; Fouché et al., 2018; Goodwin et al., 2011; Wittenberg, Alexander H J et al., 2009*) and they show a considerably lower recombination rate compared to the core chromosomes (*Croll et al., 2015; Stukenbrock and Dutheil, 2017*). However, core and supernumerary share many repetitive element families and their subtelomeric regions contain the same transposable element families (*Dhillon et al., 2014; Grandaubert et al., 2015; Schotanus et al., 2015*). In contrast to many gene-poor supernumerary chromosomes described in plants and animals, those in *Z. tritici* possess a relatively high number of protein-coding genes (727, corresponding to 6% of all genes) (*Grandaubert et al., 2015*). Recently, we demonstrated that the supernumerary chromosomes of *Z. tritici* confer a fitness cost: Isogenic strains lacking distinct supernumerary chromosomes produce higher amounts of asexual spores during host infection when compared to wild type with the complete set of supernumerary chromosomes (*Habig et al., 2017*). Despite the instability and fitness cost of the supernumerary chromosomes, they have been maintained over long evolutionary times (*Stukenbrock et al., 2011; Stukenbrock and Dutheil, 2017*), and it is therefore intriguing to address the mechanisms of supernumerary chromosome maintenance in the genome in *Z. tritici*.

Here, we used *Z. tritici* with its unique set of supernumerary chromosomes as a model to study the dynamics of unpaired chromosomes during meiosis. *Z. tritici* is a heterothallic, haploid ascomycete (i.e. two individuals of different mating type [*mat1-1* and *mat1-2*] are

required to form a diploid zygote) (*Kema et al., 1996; Kema et al., 2018*). If two haploid cells of opposite mating types contain a different complement of supernumerary chromosomes, the resulting diploid zygote consequently contains unpaired chromosomes. Upon Mendelian segregation during meiosis (segregation of the homologues chromosomes during meiosis I followed by chromatid segregation during meiosis II), four (50%) of the eight produced ascospores are predicted to contain the unpaired chromosomes (Figure 1A). To test this prediction, we performed crosses between isolates with different subsets of supernumerary chromosomes (Figure 1B). Based on controlled experiments and tetrad analyses, we surprisingly found that the supernumerary chromosomes of *Z. tritici* are subject to a meiotic drive restricted to unpaired chromosomes inherited from the female parent. Our results suggest that this drive mechanism is due to an additional, female-specific amplification of unpaired chromosomes during meiosis, a process that can ensure the maintenance of these chromosomes over long evolutionary times.

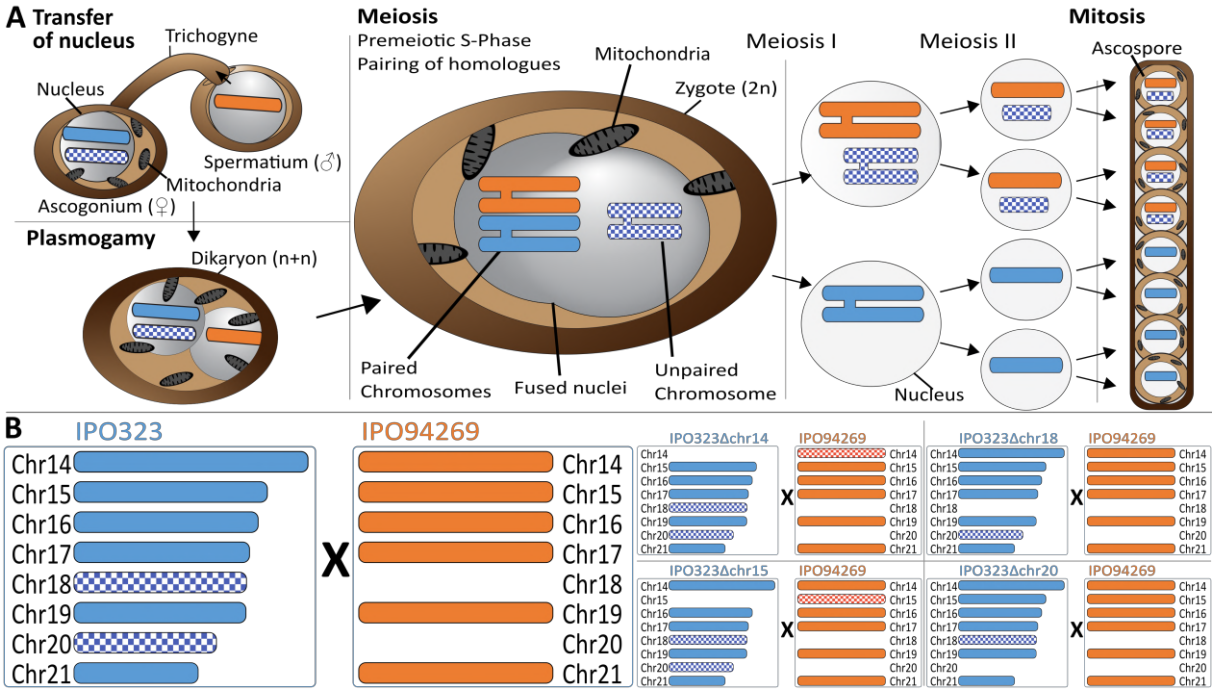

Figure 1. Meiosis and chromosome segregation in *Z. tritici*. (A) Schematic overview of the assumed sexual process between two parental strains of *Z. tritici* (*Alexopoulos and Mims; Kema et al., 2018*) with one supernumerary chromosomes shared and therefore paired (blue/orange) and one supernumerary chromosome unique to one strain (blue checkered) and unpaired in the zygote. The spermatial nucleus is transferred from the male partner via the trichogyne to the ascogonium of the female partner, resulting in plasmogamy and a dikaryon with two separate nuclei. Prior to karyogamy, the chromosomes are replicated and this comprise each two chromatids and meiosis is initiated by pairing of homologous chromosomes. In meiosis I, homologous chromosomes are segregated, followed by chromatid separation in meiosis II. A subsequent mitosis results in the production of eight ascospores contained within one ascus. The expected segregation of chromosomes according to Mendelian law of segregation is shown - which for unpaired chromosomes is 4:0. (B) Schematic illustration of the distribution of supernumerary chromosomes present in the parental strains exemplified for five of nine different crosses performed in this study. Parental strain IPO323 contains eight supernumerary chromosomes (chr14-21, blue). Parental strain IPO94269 contains six supernumerary chromosomes with homolog in IPO323 (chr14, chr15, chr16, chr17, chr19, and chr21 in orange). The IPO323 chromosomes chr18 and chr20 are not present in IPO94269. We used a set of IPO323 chromosome deletion strains to generate an additional unpaired chromosome (as example IPO323Δchr14 X IPO94269, IPO323Δchr15 X IPO94269, IPO323Δchr18 X IPO94269, IPO323Δchr20 X IPO94269 to demonstrate the one to three unpaired chromosomes and the five to six paired chromosomes present in the different crosses). Orange and blue indicate chromosomes that are shared between both strains. Checkered orange and checkered blue indicate chromosomes that are unique to one parent and therefore unpaired in the zygote.

Results

Unpaired supernumerary chromosomes show drive correlated with mitochondrial transmission. To test the transmission of supernumerary chromosomes during meiosis we used the reference strain IPO323 (mating type *mat1-1*) and eight isogenic chromosome deletion strains (IPO323Δchr14-21, mating type *mat1-1*) generated in a previous study (*Habig et al., 2017*). Each of the chromosome deletion strains differs in the absence of one supernumerary chromosome, thereby allowing us to compare the transmission of individual chromosomes in a paired and an unpaired state. We crossed these strains, *in planta,* with another *Z. tritici* isolate: IPO94269 (*mat1-2*) (Figure 1B) in three separate experiments (A, B and C) and used a combination of PCR assays, electrophoretic karyotyping and whole genome sequencing to assess the segregation of chromosomes during meiosis. IPO94269 contains six supernumerary chromosomes homologous to the IPO323 chromosomes 14, 15, 16, 17, 19, and 21 (Figure S1)(*Goodwin et al., 2011*). The experiments included a total of 39 crosses of IPO323/IPO323 chromosome deletion strains with IPO94269 resulting in different complements of paired and unpaired supernumerary chromosomes in the diploid zygote (Table 1, Table S1). We hypothesized that the inheritance of the unpaired supernumerary chromosomes could be linked to the female or male role of the parental strain. Sexual mating of heterothallic fungi of the genus *Zymoseptoria* involve a female partner that produces a sexual structure called the ascogonium. The ascogonium receives the spermatium with the male nucleus from the fertilizing male partner through a particular structure called the trichogyne (*Crous, 1998*) (Figure 1A). Importantly, the same strain can act as either the female or male partner (*Kema et al., 2018*). Mitochondrial transmission is generally associated with the female structure (*Ni et al., 2011*). We used specific mitochondrial PCR based markers to distinguish the mitochondrial genotype in the progeny and thereby determine which of the two parental strains (in this case IPO323 or IPO94269) acted as a female partner in a cross.

In all three experiments the ascospore progeny showed either the mitochondrial genotype of IPO94269 or IPO323 therefore both strains can act as the female and male partner during crosses (Table S2, S3, S4). However, transmission of the mitochondrial genotype varied significantly between experiments whereby the relative frequency of the IPO94269 mitochondrial genotype in the progeny was 80%, 11% and 65% in experiment A, B and C, respectively (Figure 2A). Interestingly, the transmission of unpaired chromosomes correlated to the sexual role (female/male) of the parent from which the unpaired chromosome was inherited. Unpaired chromosomes inherited from IPO94269 were underrepresented among ascospores with the IPO323 parent mitochondrial genotype (Figure 2B). In contrast, the unpaired supernumerary chromosomes 18 and 20, which were always inherited from the parent IPO323, were highly overrepresented among ascospores with the IPO323 mitochondrial genotype (Figure 2B). For ascospores with the mitochondrial type of the IPO94269 parent, this segregation distortion was reversed. Unpaired chromosomes inherited from IPO94269 were highly overrepresented among ascospores with the mitochondrial genotype of the IPO94269 parent. On the other hand, the unpaired supernumerary chromosomes 18 and 20, always inherited from the IPO323 parent, were underrepresented among ascospores with the mitochondrial genotype of the IPO94269 parent (Figure 2B).

Although the transmission of the supernumerary chromosomes was highly similar between experiments A, B and C when the mitochondrial genotype was used to group the data (Figure S2A), the overall transmission of the supernumerary chromosomes varied considerable between the experiments due to the highly divergent mitochondrial genotype inheritance in the three experiments (Figure S2B). However, we find a clear transmission advantage for all supernumerary chromosomes, except chromosome 14, when pooling all data from the three experiments (transmission to more than 50% of the progeny) (Figure S2C). Based on these observations, we conclude that unpaired supernumerary chromosomes show a chromosome drive mechanism, but this drive is restricted to chromosomes inherited from the mitochondria-donating female parent.

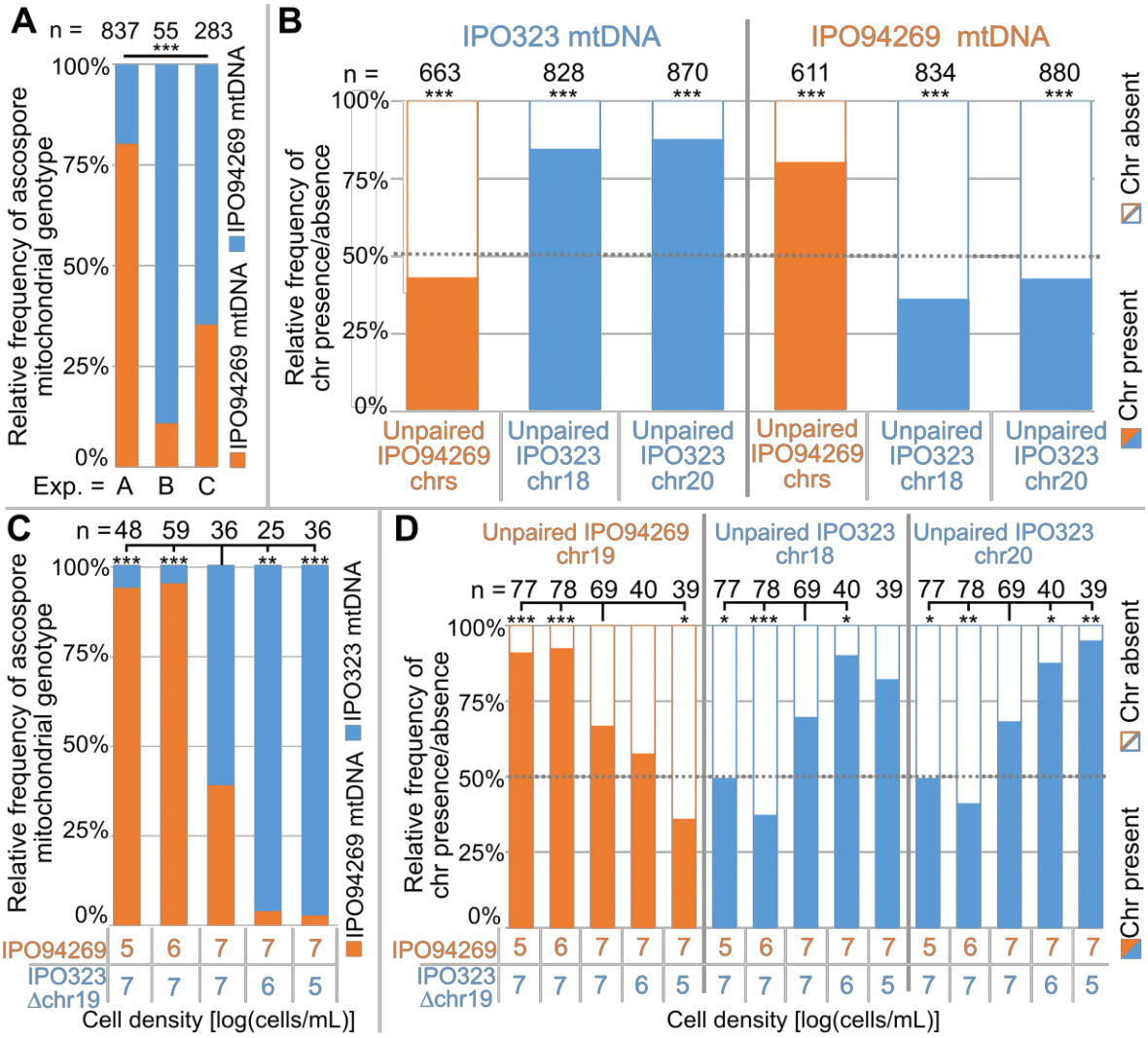

Figure 2. Unpaired supernumerary chromosomes show a segregation advantage only when inherited from the female parent. (A) Relative frequencies of mitochondrial genotypes in random and randomized ascospores in experiments A, B and C. The mitochondrial transmission varied significantly between the three experiments. Statistical significance was inferred by Fisher's exact test ($p<2.2*10^{-16}$). (B) Relative frequencies of the presence and absence of unpaired supernumerary chromosomes in all progeny ascospores pooled for experiments A, B and C according to the mitochondrial genotype of the ascospore. Orange and blue indicate unpaired chromosomes originating from IPO94269 or IPO323, respectively. For simplification the frequencies of unpaired chromosomes 14, 15, 16, 17, 19, and 21 originating from IPO94269 are pooled, while data for both unpaired chromosome 18 and 20 originating from IPO323 are depicted separately. Unpaired chromosomes inherited from the parent that provided the mitochondrial genotype (i.e. the female parent) are overrepresented in the progeny, while the same chromosomes when originating from the male parent are not. Statistical significance was inferred by a two-sided binomial test with a probability of p=0.5. (C) Cell density affects the sexual role during mating and thereby the transmission of the mitochondria. Relative frequencies of mitochondrial genotype in random and randomized ascospores isolated from crosses of IPO94269 and IPO323Δchr19 that were co-inoculated on wheat at different cell densities. The resulting progeny shows a correlation between cell-density and mitochondria transmission. Strains inoculated at lower density in general take the female role as observed by the mitochondrial transmission. Statistical significance was

inferred by a two-sided Fisher's exact test compared to the co-inoculation with equal cell densities of both strains. d) The cell density affects the transmission of unpaired chromosomes. Relative frequencies in all ascospores of the presence and absence of unpaired supernumerary chromosomes 19, inherited from parent IPO94269 and unpaired chromosomes 18 and 20, inherited from IPO323 Δchr19 are indicated according to the cell density of the parental strains IPO94269 and IPO323Δchr19 at inoculation. Statistical significance was inferred by a two-sided Fisher's exact test compared to the co-inoculation with equal cell density of both strains.(* = p<0.05, ** = p<0.005, *** = p<0.0005, see Table S5 for details on all statistical tests).

Transmission of mitochondria is affected by the cell density. We next asked which factors determine the sexual role and thereby the mitochondrial inheritance in the sexual crosses of *Z. tritici*. To this end, we considered the cell density of the two parental strains as well as the relative timing of infection as determining factors of the sexual role. To test this, we set up crosses between the strains IPO323Δchr19 and IPO94269 in which the cell density varied from 10^5 cells to 10^7 cells/mL of each of the parental strains. Furthermore, we set up crosses in which we varied the relative timing of the infection of the two parental strains to each other by inoculating one parental strain 6 or 12 days later than the other parental strain. To distinguish the female and male partner in the crosses we again assessed the mitochondrial transmission frequencies. Interestingly, we find that the cell density of the two parental strains strongly correlates with the transmission of the mitochondrial genotype. Crosses with a lower cell density of IPO323Δchr19 resulted in a higher proportion of the progeny carrying the IPO323 mitochondrial genotype (Figure 2C). Similarly, a lower cell density of IPO94269 resulted in a higher proportion of the progeny carrying the IPO94269 mitochondrial genotype. This illustrates that a density-dependent mechanism affects the sexual role of the *Z. tritici* strains during sexual mating.

Variation in the sexual role in turn affected the transmission of unpaired supernumerary chromosomes. The unpaired chromosome 19 inherited from the parent IPO94269 increased in frequency in the meiotic progeny with increasing frequency of the IPO94269 mitochondrial genotype. Unpaired chromosome 18 and chromosome 20 inherited from the parent IPO323Δchr19 increased in frequency in the meiotic progeny with an increase in frequency

of the IPO323 mitochondrial genotype (Figure 2D). Moreover, we find that the relative timing of the infection of the two strains affected the transmission of the *Z. tritici* strains. In crossing experiments where one strain was inoculated with six or twelve days delay, the later-inoculated strain more frequently exhibited the female role (Figure S2D). This could be either due to the later inoculated strain having a growth disadvantage compared to the earlier inoculated strain therefore producing a lower density of cells. This scenario would be in agreement with our observation that the parental strain with lower cell density develops the female structure (Figure 2C). Alternatively, the timing of maturation of the male and female structures might differ and possibly the female and male structures of different age could be incompatible. However, a clear effect of cell density and timing is discernable and we therefore conclude that environmental factors that affect the infection density and timing of different *Z. tritici* strain also strongly affect the sexual role of strains and thereby the transmission of supernumerary chromosomes.

Paired supernumerary chromosomes show Mendelian segregation with frequent losses. In *Z. tritici*, as in other ascomycetes, one meiosis produces eight ascospores by an additional mitosis following meiosis (*Ni et al., 2011; Wittenberg, Alexander H J et al., 2009*). The outcome of single meiotic events can be analyzed by tetrad analyses whereby the eight ascospores of a tetrad - in ascomycetes an ascus - are isolated and genotyped. We used tetrad analyses to address how paired supernumerary chromosomes segregate during meiosis. For a total of 24 separate asci, we verified that all eight ascospores originated from the same ascus and were the products of a single meiosis using six segregating markers located on the essential chromosomes (Table 2). With these 24 asci we could identify segregation patterns and furthermore eliminate post-meiotic effects on the observed chromosomal frequencies. Each tetrad allowed the analysis of the segregation pattern for both unpaired and paired chromosomes. First, we focused on the segregation of paired chromosomes within these tetrad. In the 24 asci we could observe the transmission of paired accessory chromosomes in 129 instances. We could discern the segregation of each paired supernumerary chromosome using specific segregating markers for each of the

264 supernumerary chromosomes from both parental strains. In general, the paired
265 supernumerary chromosomes showed Mendelian segregation (Figure 3). Of the 129
266 instances of supernumerary chromosome pairing, 120 (93%) showed Mendelian segregation
267 with the expected 4:4 ratio (Figure 3, black outline) and only nine instances (7%) showed a
268 deviation from the 4:4 ratio (Figure 3, red outline). In no instances did the number of
269 ascospores with a segregating marker for a paired supernumerary chromosome exceed the
270 four ascospores predicted by Mendelian segregation. In two of the nine instances however,
271 we found ascospores with two copies of supernumerary chromosome 21, representing one
272 copy from IPO323 and another from IPO94269. Whole genome sequencing validated the
273 presence of two copies of chromosome 21 in the genomes of these ascospores. In the two
274 additional ascospores of the tetrad analysis the chromosome 21 was missing (Figure S3A-C)
275 suggesting that the deviations from non-Mendelian segregation are due to loss of
276 chromosomes, non-disjunction of sister chromatids, or non-disjunction of homologous
277 chromosomes during meiosis (*Wittenberg, Alexander H J et al., 2009*).

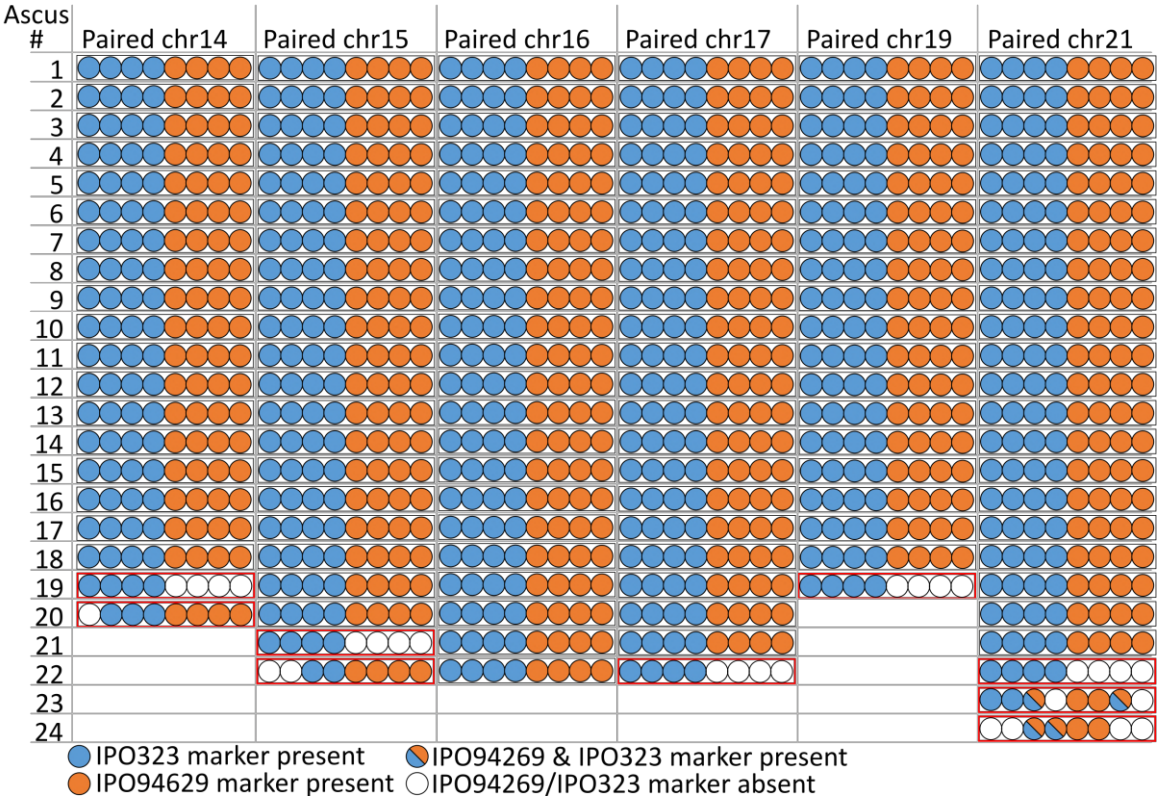

278

279 **Figure 3.** Paired supernumerary chromosomes show Mendelian segregation. Analysis of
280 segregation of paired supernumerary chromosomes in 24 complete tetrads. The

transmission of chromosomes 14, 15, 16, 17, 19, and 21 with homologs in both parental strains IPO94269 and IPO323 was detected using segregating markers for chromosomes inherited from the parental strains IPO94269 (orange) and IPO323/IPO323Δchr14-21 (blue) in the eight ascospores originating from 24 asci. In 120 of the 129 cases (black outline) we observed a 4:4 ratio in the progeny. Note: for crosses/chromosome combinations where no paired chromosome was present no ascus is shown, which reduces the number of shown asci from the 24 asci that were analyzed in both Figure 3 and Figure 4.

We next extended the analysis of transmission fidelity to include all ascospores isolated in experiments A, B and C to compare the rate of loss of paired supernumerary chromosomes. We assessed the rate of chromosome loss from 10078 instances of paired supernumerary chromosomes in isolated meiotic progenies. In 377 cases (3.7%) we found evidence for supernumerary chromosome loss in the ascospores based on the absence of specific chromosome markers (Table S6). Interestingly, the frequency of loss of paired supernumerary chromosomes varies significantly between the individual chromosomes (χ^2-Test: exp. A: $p=1.96x10^{-06}$, exp. B: $p=1.72x10^{-09}$, exp. C: $p=4.18x10^{-4}$) (Table S6) with chromosome 16 showing the lowest rate of loss in all three experiments. The frequency of chromosome loss, however, shows no correlation to particular chromosome characteristics like chromosome size or the extent of homology between the chromosomes from IPO323 and IPO94269 (Figure S1B).

Unpaired supernumerary chromosomes inherited from the female show meiotic drive. Using the same 24 complete tetrads we dissected the fate of unpaired chromosomes during single meiotic events. Each tetrad contained between one to three unpaired chromosomes with chromosome 18 and 20 being solely inherited from IPO323 and chromosome 14, 15, 16, 17, and 19 being solely inherited by the IPO94269 in crosses performed with the five IPO323 whole-chromosome-deletion strains. In contrast to paired supernumerary chromosomes, unpaired supernumerary chromosomes show distinct segregation distortion (Figure 4) that correlates with mitochondrial transmission; unpaired chromosomes originating from the female parent show a strong meiotic chromosome drive. On the other hand, unpaired

chromosomes originating from the male parent (i.e. the parent that did not provide the mitochondria) show Mendelian segregation and are more frequently lost.

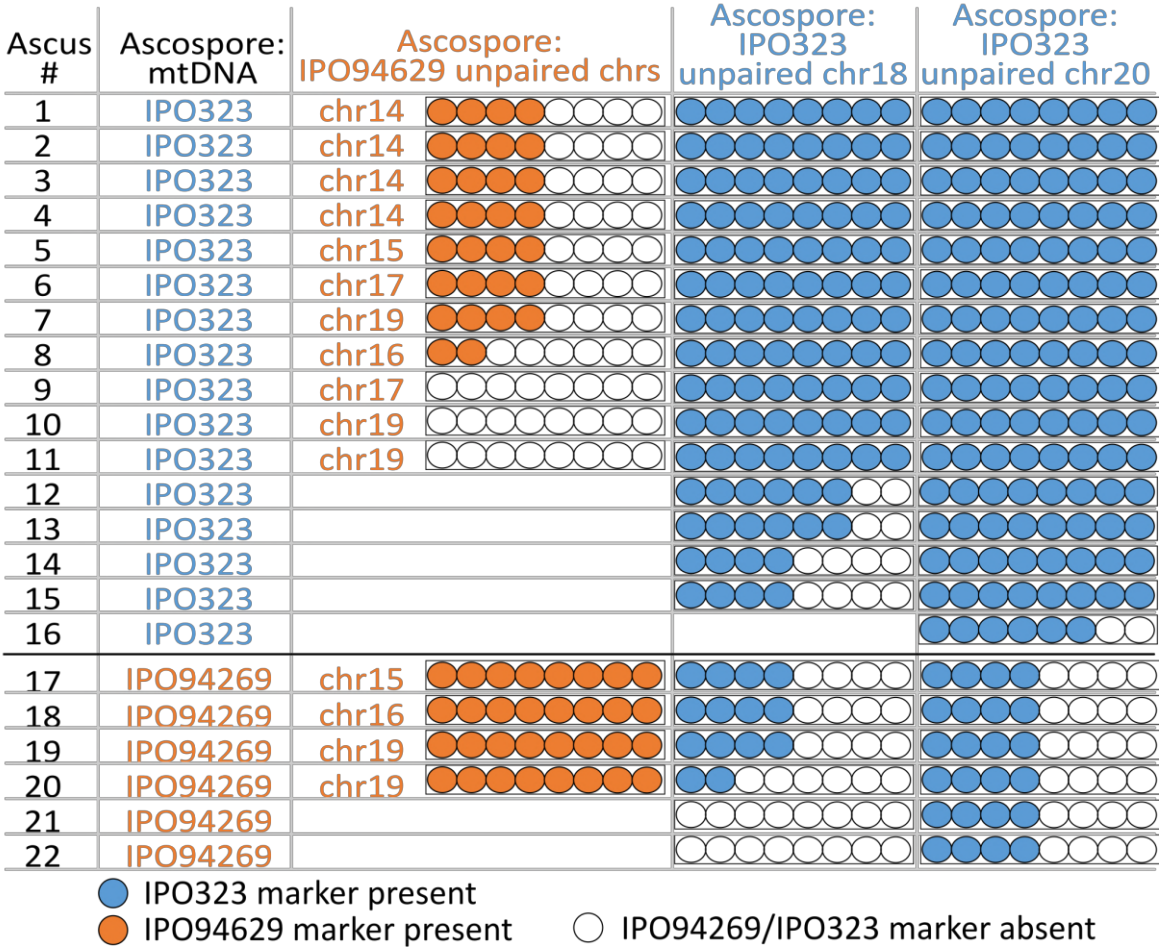

Figure 4. Unpaired supernumerary chromosome show meiotic drive if inherited from the female parent. Analysis of segregation of unpaired supernumerary chromosomes in 24 complete tetrads according to the mitochondrial genotype. The transmission of chromosomes unique to one of the parental strains and the mitochondrial genotype was detected using chromosomal or mitochondrial markers originating from IPO94269 (orange) and IPO323 (blue) in eight ascospores derived from 24 asci. When IPO323 was the female parent (i.e. the ascospores inherited the mitochondrial genotype of the IPO323 parent) unpaired chromosomes 18 and 20 originating from IPO323 show a strong chromosome drive and are overrepresented in the ascospores. When IPO94269 was the female parent unpaired chromosomes originating from IPO94269 show a strong chromosome drive. Unpaired chromosomes originating from the male parent (i.e. the one not donating the mitochondrial genotype) show Mendelian segregation or are lost. Note: for crosses/chromosome combinations where no unpaired chromosome was present no ascus is shown, which reduces the number of shown asci from the 24 asci that were analyzed in both Figure 3 and Figure 4.

In the 24 tetrads dissected here, all eight ascospores originating from the same ascus showed the same mitochondrial genotype (Table S3-S4) confirming previous results on the uniparental inheritance of mitochondria in *Z. tritici* (*Kema et al., 2018*). Isolated ascospores had the mitochondrial genotype of the parent IPO323 in 18 asci, while the ascospores of the remaining six asci showed the IPO94269 genotype, confirming that both parental strains, IPO323 and IPO94269, can act as the female parent during sexual mating with no significant difference between the two strains (two sided binomial (p=0.5), p=0.25) (*Kema et al., 2018*). In 18 asci that showed the IPO323 mitochondrial genotype, supernumerary chromosomes 18 and 20, inherited from IPO323 (the female), were unpaired in 15 and 16 meioses, respectively (Figure 4). Chromosome 18 was present in all eight ascospores in 11 of the 15 asci (ascus #1-11) instead of the expected four ascospores. In two asci, the chromosome was present in six ascospores (ascus #12-13). Chromosome 20 was present in all eight ascospores (ascus #1-15) in 15 of the 16 asci and in one ascus in six ascospores (ascus #16). This transmission pattern was reversed for the six asci exhibiting the IPO94269 mitochondrial genotype (Figure 4) Here, the female-inherited unpaired chromosomes from IPO94269 show meiotic drive while the male-inherited unpaired chromosomes from IPO323 show Mendelian segregation or were lost (Figure 4). We validated our PCR-karyotyping by sequencing the genomes of 16 ascospore isolates originating from two asci and mapped the resulting reads to the reference genome of IPO323. For all 16 ascospores we find similar coverage for all essential chromosomes and supernumerary chromosomes (Figure S3) and all 16 ascospores show similar coverage for chromosome 18 and 20 verifying the transmission of these chromosomes to the eight ascospores of each ascus instead of the expected four ascospores.

The meiotic drive of the unpaired supernumerary chromosome could imply an additional amplification step that only affects unpaired chromosomes derived from the female parent. We found however that in one cross, this additional amplification of an unpaired chromosome was incomplete: In the ascus A08-1, unpaired chromosome 18 was transmitted to all eight ascospores, but four of the ascospores contained only a partial chromosome 18, (Figure

358 S3F). The partial chromosomes 18 showed Mendelian segregation, indicating that the
359 additional amplification step of the unpaired chromosome 18 occurred prior to the first
360 meiotic division, which in this rare case was incomplete.

361

362 **Discussion**

363 The fate of supernumerary chromosomes during meiosis is poorly understood despite the
364 widespread occurrence of this type of chromosome in different taxa. Here, we show that
365 unpaired chromosomes of the fungal plant pathogen *Z. tritici* are transmitted and amplified by
366 a meiotic drive which acts only on chromosomes inherited from the female parent (Figure
367 5A). Crossing experiments of haploid individuals of opposite mating types document this as:
368 i) unpaired supernumerary chromosomes show chromosome drive only when inherited from
369 the female parent; ii) unpaired supernumerary chromosomes show Mendelian segregation
370 with frequent losses when inherited from the male parent; and iii) paired supernumerary
371 chromosomes show Mendelian segregation, but with frequent losses during meiosis.

372 Our data strongly suggest that this chromosome drive does not result from pre- or post-
373 meiotic mechanisms but occurs during meiosis. First of all, we exclude the occurrence of a
374 post-meiotic chromosome drive, e.g. killing of ascospores that did not contain the drive
375 element, as this would make it impossible to isolate complete tetrads, which we were able to.
376 Second, we consider any pre-meiotic mechanisms that could affect the number of accessory
377 chromosomes unlikely. These mechanisms could either be a premeiotic amplification (Figure
378 5B) or preferential segregation of the supernumerary chromosomes. Both mechanism would
379 affect all supernumerary chromosomes in the haploid nucleus prior to karyogamy, because
380 at this stage it not defined which of the supernumerary chromosomes will become paired and
381 which will be unpaired. Therefore, these mechanisms should always affect all supernumerary
382 chromosomes irrespective of whether they will become paired or unpaired after karyogamy.
383 If such a pre-meiotic amplification or preferential segregation would occur, the diploid zygote
384 resulting after karyogamy would be trisomic for all paired supernumerary chromosomes and

385 disomic for the unpaired chromosomes. This trisomie would result in a non-Mendelian
386 inheritance of paired supernumerary chromosomes. We did however, observe Mendelian
387 segregation for the paired supernumerary chromosomes and importantly did not find any
388 indication of additional copies of paired supernumerary chromosomes in the tetrad analysis.
389 This segregation pattern would only be possible if the additional copies of the female-
390 inherited paired supernumerary chromosomes would be lost during meiosis (Figure 5B).

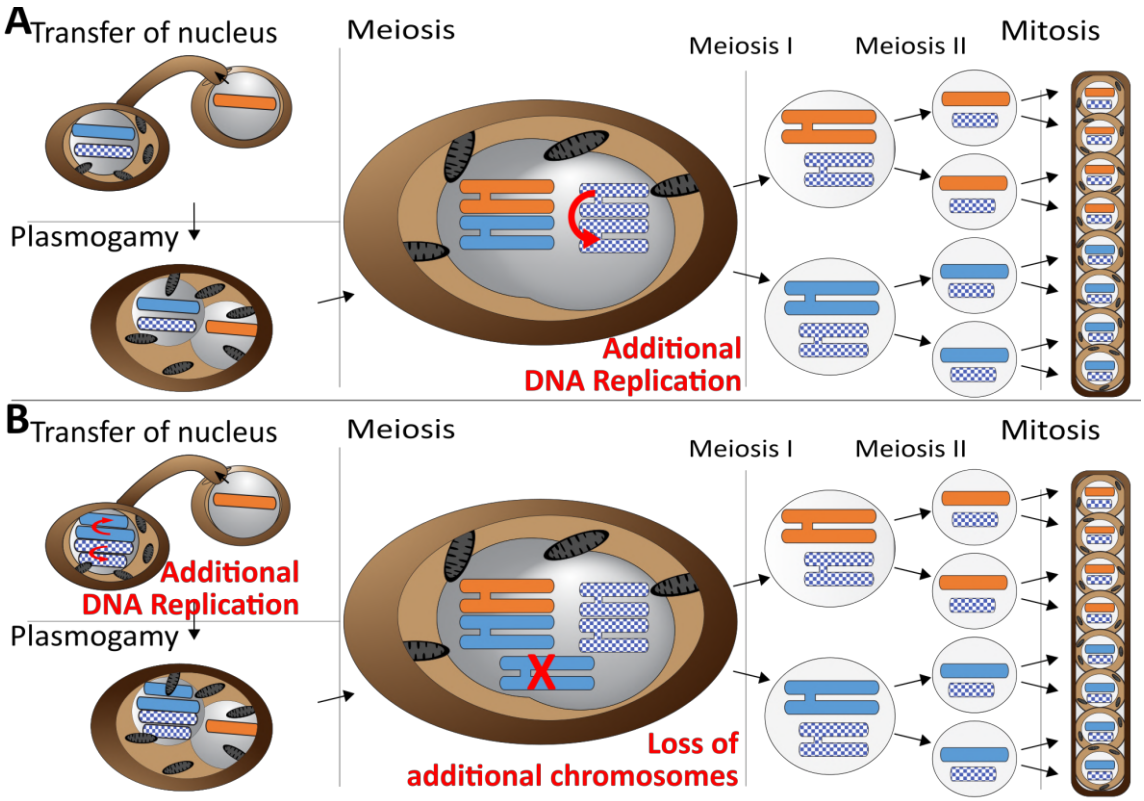

391

392 **Figure 5.** Meiotic chromosome drive in *Z. tritici*. Schematic illustration depicting two possible
393 mechanisms for the observed meiotic chromosome drive of female derived unpaired
394 supernumerary chromosomes. Light blue/orange: paired supernumerary chromosome.
395 Checkered blue: unpaired supernumerary chromosome. (A) Chromosome drive occurring
396 during meiosis, only those unpaired supernumerary chromosomes in the zygote that
397 originated from the female parent are subject to an additional round of DNA replication,
398 allowing for pairing of the two copies of the chromosome. (B) Alternative scenario under
399 which the chromosome drive occurs prior to meiosis. All supernumerary chromosomes are
400 amplified to double the copy number during development of the female ascogonium. The
401 supernumerary chromosomes are paired in the zygote during meiosis. Only additional copies
402 of the supernumerary chromosomes inherited from the female are lost while the
403 supernumerary chromosomes inherited from the male are unaffected.

404

Tightly regulated chromosome loss has been described for sex chromosomes in several insect species during embryonic development, where maternal and paternal imprinting determine the elimination of chromosomes (*Sánchez, 2014*). For *Z. tritici*, a similar mechanism would imply that all additional copies of all female supernumerary chromosomes would be eliminated during meiosis - except for the two copies of the female-inherited unpaired supernumerary chromosomes - while male supernumerary chromosomes would be unaffected. We consider this mechanism to be unlikely. In general, any pre-meiotic mechanism should affect both unpaired and paired chromosomes and therefore would require a counteracting mechanism after karyogamy that results in the Mendelian Segregation pattern observed in the paired supernumerary chromosomes. Instead, we propose that an additional amplification affecting only female-inherited supernumerary chromosomes could be a plausible scenario explaining the observed meiotic drive of supernumerary chromosomes in *Z. tritici* during sexual mating. The additional amplification of unpaired supernumerary chromosomes would require an additional initiation of DNA-replication restricted to unpaired chromosomes and therefore a feedback between pairing of homologous chromosomes and DNA replication. Although DNA-replication is a highly regulated process and any feedback from chromosome pairing is currently unknown, we suggest that this model is the most likely to explain the observed pattern. Feedback between meiotic S-phase and the pairing of homologous chromosomes has been proposed based on the effects of interchromosomal interaction proteins like Spo11 - a key mediator of interhomolog interactions that is responsible for the initiation of meiotic recombination - on the progression of meiotic DNA replication (*Cha et al., 2000*). Although Spo11 cannot explain the additional amplification of unpaired chromosomes it highlights a potential for a feedback between pairing of homologues and DNA-replication. In addition, pairing of homologous chromosomes or sequences has also been described for somatic cells in *Saccharomyces cerevisiae, Schizosaccharomyces pombe* and *Drosophila melanogaster* highlighting the possible existence of homologues pairing prior to DNA-replication (*Burgess et al., 1999; Dernburg et al., 1996; Joyce et al., 2013; Scherthan et al., 1994; Weiner and Kleckner,*

433 *1994*). We therefore consider it possible that meiosis in *Z. tritici* involves an additional
434 feedback mechanism that induces an additional round of amplification based on the unpaired
435 chromosome status.

436 A meiotic chromosome drive can explain the continued maintenance of supernumerary
437 chromosomes in *Z. tritici* despite the negative effects on fitness during host infection (*Habig*
438 *et al., 2017*). However, it is unclear how this type of chromosome drive can act
439 simultaneously on several separate chromosomes. In our experiments, we found that seven
440 of the eight supernumerary chromosomes showed drive, and we hypothesize that the drive
441 mechanism (i.e., the additional amplification of the unpaired female supernumerary
442 chromosomes) depends on a general characteristic of the supernumerary chromosomes.
443 Interestingly, we observed the meiotic drive of unpaired accessory chromosomes for 7 of the
444 8 accessory chromosomes of the reference isolate IPO323. Chr14 for which no such
445 transmission advantage was observed, is the largest of the accessory chromosomes (773
446 kb) in IPO323 (*Goodwin et al., 2011*). A large insertion spanning approx. 400 kb in chr14
447 shows presence/absence polymorphism in *Z. tritici* resulting in isolates that contain a much
448 smaller chr14 (*Croll et al., 2013*). Interestingly the smaller chr14 showed a transmission
449 advantage when present in one the parental strains in a previous study (*Croll et al., 2013*),
450 which could point to chromosome size as a factor influencing the observed drive.

451 Currently, we cannot explain why the hypothesized additional amplification of the
452 supernumerary chromosome is restricted to unpaired chromosomes inherited from the
453 female parent. In ascomycetes, plasmogamy and karyogamy are separated by a dikaryon
454 stage, in which the female and male nuclei are separate (*Ni et al., 2011*). Consequently,
455 there is a temporal separation of the processes determining uniparental inheritance of the
456 mitochondria, nuclear inheritance, and the proposed additional amplification of the unpaired
457 supernumerary chromosomes. Female chromosome drive in the fungus would depend on a
458 female-derived signal that persists through plasmogamy to karyogamy when DNA

amplification takes place. We currently do not know the nature of this signal, but speculate that it could be mediated by epigenetic mechanisms similar to genomic imprinting.

In this study, we have shown that supernumerary chromosomes of *Z. tritici* are subjected to a meiotic drive, which is probably dependent on an additional meiotic amplification of unpaired chromosomes. This mechanism may explain the continued maintenance of supernumerary chromosomes in *Z. tritici* over long evolutionary times in spite of their frequent loss during mitosis and their fitness cost during plant infection and asexual propagation.

Materials and Methods

Fungal and plant material. The Dutch isolates IPO323 and IPO94269 are available from the Westerdijk Institute (Utrecht, The Netherlands) with the accession numbers CBS115943 and CBS115941. *Triticum aestivum* cultivar Obelisk used for the *in planta* fungal mating was obtained from Wiersum Plantbreeding BV (Winschoten, The Netherlands). Sexual crosses were conducted as described in (*Kema et al., 1996; Kema et al., 2018*).

Fungal growth conditions. IPO94269 was maintained in liquid yeast glucose (YG) broth (30 g/L glucose and 10 g/L yeast extract) at 15°C on an orbital shaker. Due to their tendency to form hyphal lumps in liquid media IPO323 and IPO323-derived whole chromosome deletion strains and all progeny were maintained on solid YMS (4 g/L yeast extract, 4 g/L malt extract, 4 g/L sucrose, and 20 g/L agar) at 18°C. For infection cells were washed once and diluted in H_2O including 0.05% Tween20 to the indicated cell density.

Sexual mating of Z. tritici strains. Sexual crosses were performed as previously described in (*Kema et al., 1996; Kema et al., 2018*). In short: 11-14 day old wheat plants were infected by spraying until droplets run-off the leaf surface. Plants were kept at 100% humidity for 48 hours before placing them for 12 hours at 90% humidity and 16 hours light days. At day 14 post infection all except the first leaf of each plants were removed, the plants transferred to buckets with fertilized soil, and the buckets put into coarse netting, placed outside and

485 regularly watered. Seven to eleven weeks after infection infected leaves were harvested
486 weekly and placed in tap water over night at room temperature. The infected leaves were
487 placed on wet filter paper occupying ¼ of a Petri dish lid, excessive water removed and a
488 Petri dish containing 2% water agar (WA) was placed on top to collect the forcefully ejected
489 ascospores. Every 10 min for a total of 80 min the water agar containing petri dish was
490 rotated by 45° to collect the ejected ascospores. The WA plates were incubated for 18-24h at
491 room temperature and ascospores were counted by visual inspection using a dissecting
492 stereo microscope. A total of 39 independent crosses were conducted for this study. Table 1
493 provides a summary of the crosses performed and the verified progeny obtained within these
494 crosses.

495

Table 1. Summary of crosses and progeny generated in this study

						Ascospores (random*/all)			Verified tetrads (mtIPO323/mtIPO94269)		
#	Parental strain 1	Parental strain 2	Unpaired chr from IPO94269	Unpaired chr from IPO323	Condition	Exp A	Exp B	Exp C	Exp A	Exp B	Exp C
1	IPO323	IPO94269	-	chr18, chr20	Co-inoculation 10^7 cells/mL	96/96	12/96	51/88	-	2/2	0
2	IPO323 Δchr14	IPO94269	chr14	chr18, chr20	Co-inoculation 10^7 cells/mL	96/96	8/64	38/72	-	3/0	1/0
3	IPO323 Δchr21	IPO94269	chr21	chr18, chr20	Co-inoculation 10^7 cells/mL	89/89	4/32	52/78	-	0	0
4	IPO323 Δchr16	IPO94269	chr16	chr18, chr20	Co-inoculation 10^7 cells/mL	96/96	6/48	38/115	-	1/0	0/1
5	IPO323 Δchr17	IPO94269	chr17	chr18, chr20	Co-inoculation 10^7 cells/mL	96/96	2/16	15/59	-	0	2/0
5	IPO323 Δchr19	IPO94269	chr19	chr18, chr20	Co-inoculation 10^7 cells/mL	96/96	9/72	38/77	-	3/1	0/1
7	IPO323 Δchr20	IPO94269	-	chr18	Co-inoculation 10^7 cells/mL	96/96	4/32	19/31	-	2/0	0
8	IPO323 Δchr18	IPO94269	-	chr20	Co-inoculation 10^7 cells/mL	96/96	4/32	30/67	-	1/0	2/0
9	IPO323 Δchr15	IPO94269	chr15	chr18, chr20	Co-inoculation 10^7 cells/mL	96/96	6/48	14/54	-	1/0	0/1
10	IPO323 Δchr19	IPO94269	chr19	chr18, chr20	IPO323 10^6 cells/mL	-	-	25/42	-	-	0
11	IPO323 Δchr19	IPO94269	chr19	chr18, chr20	IPO323 10^5 cells/mL	-	-	38/43	-	-	0
12	IPO323 Δchr19	IPO94269	chr19	chr18, chr20	IPO323 10^4 cells/mL	-	-	2/16	-	-	0
13	IPO323 Δchr19	IPO94269	chr19	chr18, chr20	IPO94269 +6dpi	-	-	40/46	-	-	0
14	IPO323 Δchr19	IPO94269	chr19	chr18, chr20	IPO94269 +12dpi	-	-	11/11	-	-	0
15	IPO323 Δchr19	IPO94269	chr19	chr18, chr20	IPO94269 10^6 cells/mL	-	-	60/84	-	-	0
16	IPO323 Δchr19	IPO94269	chr19	chr18, chr20	IPO94269 10^5 cells/mL	-	-	48/80	-	-	0
17	IPO323 Δchr19	IPO94269	chr19	chr18, chr20	IPO94269 10^4 cells/mL	-	-	28/28	-	-	0
18	IPO323 Δchr19	IPO94269	chr19	chr18, chr20	IPO323 +6pdi	-	-	5/29	-	-	0
19	IPO323 Δchr19	IPO94269	chr19	chr18, chr20	IPO323 +12dpi	-	-	51/71	-	-	1/0
					∑	**761/761**	**55/440**	**603/1091**	**-**	**13/3**	**5/3**

* Includes random and randomized ascospores. Randomized asocpsores were generated by randomly selecting one ascopore per tetrad.

Ascospore isolation and ascus verification

Ascospores were isolated from the WA 18-28h after ejection from the ascus using a dissecting stereo microscope and a sterile syringe needle, placed onto YMS plates and grown for 6-7days at 18°C. One colony per isolated ascospore was streaked out on YMS plates and grown again for 6-7 days at 18°C. Single colonies were isolated and used for all

505 further characterisation. To isolate all ascospore from an ascus eight germinated ascospores
506 that were spatially separate on the WA were considered to be ejected from one ascus. All
507 eight ascospores were isolated.

508 To verify that the eight ascospores originated from the same ascus, the following six
509 segregating markers located on the essential chromosomes were used: *mat1-1*/*mat1-2*
510 (*Waalwijk et al., 2002*), 11O21, 04L20, caa-0002, ggc-001 and ac-0001 (*Goodwin et al.,*
511 *2007*) (Table 2).

512 **Table 2.** Overview of six segregating markers located on the essential chromosomes.

Marker	Primer1	Primer 2	Product size in IPO323 [bp]	Product size in IPO94269 [bp]
mat1-1/*mat1-2*	MAT1-1F, MAT1-1R	MAT1-2F, MAT1-2R	340	660
11O21	11O21F	11O21R	205	199
04L20	04L20F	04L20R	192	199
caa-0002	2996	2997	412	396
ggc-001	2998	2999	254	234
ac-0001	3000	3001	187	173

513

514 Only when i) all eight ascospores from one putative ascus showed a 4:4 ratio based on the
515 amplification of these markers AND ii) exactly two ascospores were twins, we considered the
516 ascospores to be derived from one ascus. As an internal PCR control an amplification of the
517 *gapdh* (primer: 879, 880) was used to verify negative PCR results.

518 In experiment B a total of 440 ascospores were isolated from 55 asci, and of these, 128
519 ascospores from 16 asci met the criteria and were considered to be derived from within one
520 ascus. In experiment C a total of 504 ascospores were isolated from a total of 63 asci, and of
521 these, 64 of eight asci met these criteria. The mitochondrial genotype was determined using
522 the primers Mt-SSR-F and Mt-SSR-R (*Kema et al., 2018*).

Ascospores were karyotyped for the presence of supernumerary chromosomes using primer pairs specifically designed to test for the presence of chromosomes 14, 15, 16, 17, 18, 19, 20, and 21 derived from IPO323 and from IPO94269 (Table S1, Figure S4) using standard conditions (*Habig et al., 2017*). For unpaired chromosomes that were overrepresented in the ascospores of experiment B and C, we validated their presence by two additional PCRs that amplify a sequence in the right subtelomeric and left subtelomeric regions of the chromosome (Table S1, Figure S4). For paired supernumerary chromosomes, we designed the primers to reveal a size difference in the amplification products of IPO323-derived and IPO94269-derived chromosomes (Table S1, Figure S4). In addition, verification of the karyotype was conducted using a pulsed-field gel electrophoresis system as described previously (*Habig et al., 2017*) (Figure S5).

Statistical analysis. All statistical analyses were conducted in R (version R3.4.1) (*R Core Team, 2015*) using the suite R Studio (version 1.0.143) (*RStudio Team, 2015*). Two-sided Fisher's exact tests were performed at a confidence level of 0.95. Due to the codependency of mitochondrial data of ascospores isolated from a potential or verified ascus, due to the fact that all asospores of an ascus will receive the same mitochondrial genotype, one asopore from each potential and verified ascus was randomly selected and included in the statistical analysis of the mitochondrial genotype transmission. For large datasets the Fisher's exact test was replaced by the Pearson's Chi-squared test. Two-sided binomial tests were performed with a hypothesized probability of p=0.5 at a confidence level of 0.95 on all statistical analysis on a deviation of an assumed Mendelian segregation of unpaired supernumerary chromosomes which would be predicted to be present in 50% of the progeny. All statistical analysis on transmission of supernumerary chromosomes included all randomly selected ascospores as well as all ascospores selected from potential and verified asci.

Genome sequencing. For sequencing, DNA of IPO94269 and 16 ascospores was isolated using a phenol-chloroform extraction protocol as described previously (*Sambrook and Russell, 2001*). Library preparation and sequencing using a Pacific Biosciences Sequel for

IPO94269 and Illumina HiSeq3000 machine for 16 ascospore-derived colonies were performed at the Max Planck Genome Centre, Cologne, Germany. Reads have been deposited in the Sequence Read Archive and are available under the BioProject PRJNA438050. Assembly of the IPO94269 genome was conducted at the Max Planck Genome Center, Cologne using the software suite HGAP 4 (*Chin et al., 2016*) from Pacific Biosciences using the default settings. Synteny analysis was conducted with SyMAP version 4.2 (*Soderlund et al., 2006; Soderlund et al., 2011*) (Figure S5). Illumina reads of the ascospores were filtered and mapped to the reference genome of IPO323 (*Goodwin et al., 2011*) as previously described (*Habig et al., 2017*) in which the transposable elements were masked (*Grandaubert et al., 2015*).

Reference mapping of Illumina reads. Paired-end reads of 150 bp were mapped directly to the genome of the reference isolate IPO323 (*Goodwin et al., 2011*). Processing of the reads were carried out using the below listed pipeline:

1) Quality filtering using Trimmomatic V0.30 (*Bolger et al., 2014*)

```
java -jar /trimmomatic-0.30.jar PE -phred33 R1.fastq R2.fastq R1_paired.fastq
R1_unpaired.fastq R2_paired.fastq R2_unpaired.fastq HEADCROP:2 CROP:149
LEADING:3 TRAILING:3 SLIDINGWINDOW:4:15 MINLEN:50
```

http://www.usadellab.org/cms/?page=trimmomatic

2) Mapping to IPO323 reference genome using Bowtie 2 version 2.1.0 (*Langmead and Salzberg, 2012*)

```
bowtie2 -p 6 -q -x IPO323_reference -1 R1_paired.fastq -2 R2_paired.fastq -S R.sam
```

http://bowtie-bio.sourceforge.net/bowtie2/index.shtml

3) Converting to BAM and sorting using Picard 1.141

```
java -jar /picard.jar SortSam INPUT=R.sam OUTPUT=R.bam SORT_ORDER=coordinate
```

http://broadinstitute.github.io/picard

References

Akera T, Chmátal L, Trimm E, Yang K, Aonbangkhen C, Chenoweth DM, Janke C, Schultz RM, Lampson MA. 2017. Spindle asymmetry drives non-Mendelian chromosome segregation. *Science (New York, N.Y.)* **358**:668–672. doi: 10.1126/science.aan0092.

Alexopoulos CJ, Mims CW. Blackwell. M. 1996. *Introductory Mycology. 4th ed. John Wiley & Sons, New York, USA, 869pp*.

Bolger AM, Lohse M, Usadel B. 2014. Trimmomatic: a flexible trimmer for Illumina sequence data. *Bioinformatics (Oxford, England)* **30**:2114–2120. doi: 10.1093/bioinformatics/btu170.

Burgess SM, Kleckner N, Weiner BM. 1999. Somatic pairing of homologs in budding yeast: Existence and modulation. *Genes & development* **13**:1627–1641.

Cha RS, Weiner BM, Keeney S, Dekker J, Kleckner N. 2000. Progression of meiotic DNA replication is modulated by interchromosomal interaction proteins, negatively by Spo11p and positively by Rec8p. *Genes & development* **14**:493–503.

Chin C-S, Peluso P, Sedlazeck FJ, Nattestad M, Concepcion GT, Clum A, Dunn C, O'Malley R, Figueroa-Balderas R, Morales-Cruz A, Cramer GR, Delledonne M, Luo C, Ecker JR, Cantu D, Rank DR, Schatz MC. 2016. Phased diploid genome assembly with single-molecule real-time sequencing. *Nature methods* **13**:1050–1054. doi: 10.1038/nmeth.4035.

Croll D, Lendenmann MH, Stewart E, McDonald BA. 2015. The Impact of Recombination Hotspots on Genome Evolution of a Fungal Plant Pathogen. *Genetics* **201**:1213–1228. doi: 10.1534/genetics.115.180968.

Croll D, Zala M, McDonald BA, Heitman J. 2013. Breakage-fusion-bridge Cycles and Large Insertions Contribute to the Rapid Evolution of Accessory Chromosomes in a Fungal Pathogen. *PLoS Genetics* **9**:e1003567. doi: 10.1371/journal.pgen.1003567.

Crous PW. 1998. *Mycosphaerella spp. and their anamorphs associated with leaf spot diseases of Eucalyptus*. American Phytopathological Society (APS Press).

Dernburg AF, Sedat JW, Hawley RS. 1996. Direct evidence of a role for heterochromatin in meiotic chromosome segregation. *Cell* **86**:135–146.

603 **Dhillon B**, Gill N, Hamelin RC, Goodwin SB. 2014. The landscape of transposable elements
604 in the finished genome of the fungal wheat pathogen Mycosphaerella graminicola. *BMC*
605 *genomics* **15**:1132. doi: 10.1186/1471-2164-15-1132.
606 **Fouché S**, Plissonneau C, McDonald BA, Croll D. 2018. Meiosis leads to pervasive copy-
607 number variation and distorted inheritance of accessory chromosomes of the wheat
608 pathogen Zymoseptoria tritici. *Genome biology and evolution* **10**:1416–1429.
609 **Goodwin SB**, Ben M'Barek S, Dhillon B, Wittenberg, Alexander H. J., Crane CF, Hane JK,
610 Foster AJ, Van der Lee, Theo A. J., Grimwood J, Aerts A, Antoniw J, Bailey A, Bluhm B,
611 BOWLER J, Bristow J, van der Burgt, Ate, Canto-Canché B, Churchill, Alice C. L., Conde-
612 Ferràez L, Cools HJ, Coutinho PM, CSUKAI M, Dehal P, Wit P de, Donzelli B, van de
613 Geest, Henri C., van Ham, Roeland C. H. J., Hammond-Kosack KE, Henrissat B, Kilian A,
614 Kobayashi AK, Koopmann E, Kourmpetis Y, Kuzniar A, Lindquist E, Lombard V,
615 Maliepaard C, Martins N, Mehrabi R, Nap, Jan P. H., Ponomarenko A, Rudd JJ, Salamov
616 A, Schmutz J, Schouten HJ, Shapiro H, Stergiopoulos I, Torriani, Stefano F. F., Tu H, de
617 Vries, Ronald P., Waalwijk C, Ware SB, Wiebenga A, Zwiers L-H, Oliver RP, Grigoriev IV,
618 Kema, Gert H. J., Malik HS. 2011. Finished Genome of the Fungal Wheat Pathogen
619 Mycosphaerella graminicola Reveals Dispensome Structure, Chromosome Plasticity, and
620 Stealth Pathogenesis. *PLoS Genetics* **7**:e1002070. doi: 10.1371/journal.pgen.1002070.
621 **Goodwin SB**, **Van der Lee, Theo A. J.**, Cavaletto JR, Te Lintel Hekkert B, Crane CF,
622 **Kema, Gert H. J.** 2007. Identification and genetic mapping of highly polymorphic
623 microsatellite loci from an EST database of the septoria tritici blotch pathogen
624 Mycosphaerella graminicola. *Fungal genetics and biology : FG & B* **44**:398–414.
625 doi: 10.1016/j.fgb.2006.09.004.
626 **Grandaubert J**, Bhattacharyya A, Stukenbrock EH. 2015. RNA-seq based gene annotation
627 and comparative genomics of four fungal grass pathogens in the genus Zymoseptoria
628 identify novel orphan genes and species-specific invasions of transposable elements. *G3*
629 *(Bethesda, Md.)* g3. 115.017731.

630 **Habig M**, Quade J, Stukenbrock EH. 2017. Forward Genetics Approach Reveals Host
631 Genotype-Dependent Importance of Accessory Chromosomes in the Fungal Wheat
632 Pathogen Zymoseptoria tritici. *mBio* **8**:e01919-17. doi: 10.1128/mBio.01919-17.
633 **Hasegawa N**. 1934. A Cytological Study on 8-Chromosome Rye. *CYTOLOGIA* **6**:68–77.
634 doi: 10.1508/cytologia.6.68.
635 **Houben A**. 2017. B Chromosomes - A Matter of Chromosome Drive. *Frontiers in plant*
636 *science* **8**:210. doi: 10.3389/fpls.2017.00210.
637 **Houben A**, Banaei-Moghaddam AM, Klemme S, Timmis JN. 2014. Evolution and biology of
638 supernumerary B chromosomes. *Cellular and Molecular Life Sciences* **71**:467–478.
639 doi: 10.1007/s00018-013-1437-7.
640 **Jones RN**. 1995. Tansley review no. 85. B chromosomes in plants. *New Phytologist* 411–
641 434.
642 **Jones RN**, Viegas W, Houben A. 2008. A century of B chromosomes in plants: so what?
643 *Annals of botany* **101**:767–775. doi: 10.1093/aob/mcm167.
644 **Joyce EF**, Apostolopoulos N, Beliveau BJ, Wu C-t. 2013. Germline progenitors escape the
645 widespread phenomenon of homolog pairing during Drosophila development. *PLoS*
646 *genetics* **9**:e1004013. doi: 10.1371/journal.pgen.1004013.
647 **Kema GH**, Verstappen EC, Todorova M, Waalwijk C. 1996. Successful crosses and
648 molecular tetrad and progeny analyses demonstrate heterothallism in Mycosphaerella
649 graminicola. *Current genetics* **30**:251–258.
650 **Kema GHJ**, Gohari AM, Aouini L, Gibriel HAY, Ware SB, van den Bosch, Frank, Manning-
651 Smith R, Alonso-Chavez V, Helps J, M'Barek SB. 2018. Stress and sexual reproduction
652 affect the dynamics of the wheat pathogen effector AvrStb6 and strobilurin resistance.
653 *Nature genetics* **50**:375.
654 **Klutstein M**, Cooper JP. 2014. The Chromosomal Courtship Dance-homolog pairing in early
655 meiosis. *Current opinion in cell biology* **26**:123–131. doi: 10.1016/j.ceb.2013.12.004.
656 **Langmead B**, Salzberg SL. 2012. Fast gapped-read alignment with Bowtie 2. *Nature*
657 *methods* **9**:357–359. doi: 10.1038/nmeth.1923.

658 **Levin DA**, Palestis BG, Jones RN, Trivers R. 2005. Phyletic hot spots for B chromosomes in
659 angiosperms. *Evolution* **59**:962–969.
660 **Loidl J**. 2016. Conservation and Variability of Meiosis Across the Eukaryotes. *Annual review*
661 *of genetics* **50**:293–316. doi: 10.1146/annurev-genet-120215-035100.
662 **Ma L-J**, **van der Does, H Charlotte**, Borkovich KA, Coleman JJ, Daboussi M-J, Di Pietro A,
663 Dufresne M, Freitag M, Grabherr M, Henrissat B, Houterman PM, Kang S, Shim W-B,
664 Woloshuk C, Xie X, Xu J-R, Antoniw J, Baker SE, Bluhm BH, Breakspear A, Brown DW,
665 **Butchko, Robert A E**, Chapman S, Coulson R, Coutinho PM, Danchin, Etienne G J,
666 Diener A, Gale LR, Gardiner DM, Goff S, Hammond-Kosack KE, Hilburn K, Hua-Van A,
667 Jonkers W, Kazan K, Kodira CD, Koehrsen M, Kumar L, Lee Y-H, Li L, Manners JM,
668 Miranda-Saavedra D, Mukherjee M, Park G, Park J, Park S-Y, Proctor RH, Regev A, Ruiz-
669 Roldan MC, Sain D, Sakthikumar S, Sykes S, Schwartz DC, Turgeon BG, Wapinski I,
670 Yoder O, Young S, Zeng Q, Zhou S, Galagan J, Cuomo CA, Kistler HC, Rep M. 2010.
671 Comparative genomics reveals mobile pathogenicity chromosomes in Fusarium. *Nature*
672 **464**:367–373. doi: 10.1038/nature08850.
673 **Miao V**, Covert S, VanEtten H. 1991. A fungal gene for antibiotic resistance on a dispensable
674 (\"B\") chromosome. *Science* **254**:1773–1776. doi: 10.1126/science.1763326.
675 **Moeller M**, Habig M, Freitag M, Stukenbrock EH. 2018. Extraordinary genome instability and
676 widespread chromosome rearrangements during vegetative growth. *bioRxiv* 304915.
677 **Mroczek RJ**, Melo JR, Luce AC, Hiatt EN, Dawe RK. 2006. The maize Ab10 meiotic drive
678 system maps to supernumerary sequences in a large complex haplotype. *Genetics*
679 **174**:145–154. doi: 10.1534/genetics.105.048322.
680 **Ni M**, Feretzaki M, Sun S, Wang X, Heitman J. 2011. Sex in fungi. *Annual review of genetics*
681 **45**:405–430. doi: 10.1146/annurev-genet-110410-132536.
682 **Ohta S**. 1996. Mechanisms of B-chromosome accumulation in Aegilops mutica Boiss. *Genes*
683 *& Genetic Systems* **71**:23–29. doi: 10.1266/ggs.71.23.
684 **Plissonneau C**, Stürchler A, Croll D. 2016. The evolution of orphan regions in genomes of a
685 fungal pathogen of wheat. *mBio* **7**:e01231-16.

686 **R Core Team**. 2015. *R: A Language and Environment for Statistical Computing*. Vienna,
687 Austria.
688 **RStudio Team**. 2015. *RStudio: Integrated Development Environment for R*. Boston, MA.
689 **Sambrook J**, Russell DW. 2001. *Molecular Cloning: A laboratory manual, 3rd edn.* Gold
690 Spring Harbor Laboratory Pr, Gold Spring Harbor, New York.
691 **Sánchez L**. 2014. Sex-determining mechanisms in insects based on imprinting and
692 elimination of chromosomes. *Sexual development : genetics, molecular biology, evolution,*
693 *endocrinology, embryology, and pathology of sex determination and differentiation* **8**:83–
694 103. doi: 10.1159/000356709.
695 **Scherthan H**, Bähler J, Kohli J. 1994. Dynamics of chromosome organization and pairing
696 during meiotic prophase in fission yeast. *The Journal of cell biology* **127**:273–285.
697 **Schotanus K**, Soyer JL, Connolly LR, Grandaubert J, Happel P, Smith KM, Freitag M,
698 Stukenbrock EH. 2015. Histone modifications rather than the novel regional centromeres
699 of Zymoseptoria tritici distinguish core and accessory chromosomes. *Epigenetics &*
700 *chromatin* **8**:41. doi: 10.1186/s13072-015-0033-5.
701 **Soderlund C**, Bomhoff M, Nelson WM. 2011. SyMAP v3.4: A turnkey synteny system with
702 application to plant genomes. *Nucleic acids research* **39**:e68. doi: 10.1093/nar/gkr123.
703 **Soderlund C**, Nelson W, Shoemaker A, Paterson A. 2006. SyMAP: A system for discovering
704 and viewing syntenic regions of FPC maps. *Genome Research* **16**:1159–1168.
705 doi: 10.1101/gr.5396706.
706 **Stukenbrock EH**, Bataillon T, Dutheil JY, Hansen TT, Li R, Zala M, McDonald BA, Wang J,
707 Schierup MH. 2011. The making of a new pathogen: Insights from comparative population
708 genomics of the domesticated wheat pathogen Mycosphaerella graminicola and its wild
709 sister species. *Genome Research* **21**:2157–2166. doi: 10.1101/gr.118851.110.
710 **Stukenbrock EH**, Dutheil JY. 2017. Fine-Scale Recombination Maps of Fungal Plant
711 Pathogens Reveal Dynamic Recombination Landscapes and Intragenic Hotspots.
712 *Genetics*. doi: 10.1534/genetics.117.300502.

713 **Valente GT**, Nakajima RT, Fantinatti BEA, Marques DF, Almeida RO, Simões RP, Martins C.
714 2017. B chromosomes: From cytogenetics to systems biology. *Chromosoma* **126**:73–81.
715 doi: 10.1007/s00412-016-0613-6.
716 **Waalwijk C**, Mendes O, Verstappen ECP, Waard MA de, Kema, Gert H. J. 2002. Isolation
717 and characterization of the mating-type idiomorphs from the wheat septoria leaf blotch
718 fungus Mycosphaerella graminicola. *Fungal genetics and biology : FG & B* **35**:277–286.
719 doi: 10.1006/fgbi.2001.1322.
720 **Weiner BM**, Kleckner N. 1994. Chromosome pairing via multiple interstitial interactions
721 before and during meiosis in yeast. *Cell* **77**:977–991.
722 **Wittenberg, Alexander H J**, **van der Lee, Theo A J**, Ben M'Barek S, Ware SB, Goodwin
723 SB, Kilian A, Visser, Richard G F, Kema, Gert H J, Schouten HJ. 2009. Meiosis drives
724 extraordinary genome plasticity in the haploid fungal plant pathogen Mycosphaerella
725 graminicola. *PloS one* **4**:e5863. doi: 10.1371/journal.pone.0005863.
726 **Zickler D**, Kleckner N. 2015. Recombination, Pairing, and Synapsis of Homologs during
727 Meiosis. *Cold Spring Harbor perspectives in biology* **7**. doi: 10.1101/cshperspect.a016626.
728

729 ## Acknowledgments

730 The authors thank Michael Freitag and members of the Environmental Genomics group for
731 helpful discussions and Diethard Tautz for comments to a previous version of this
732 manuscript. The study was funded by a personal grant to EHS from the State of Schleswig
733 Holstein and the Max Planck Society. The funders had no role in study design, data
734 collection and interpretation, or the decision to submit the work for publication.

735

736 ## Competing interests

737 The authors declare no competing interests.

738

Author contributions

MH: Conceptualization, Investigation, Formal analysis, Visualization, Writing-original draft

GHJK: Conceptualization, Writing-review & editing, Supervision

EHS: Conceptualization, Writing-review & editing, Supervision, Project administration, Funding acquisition

Supplementary figures

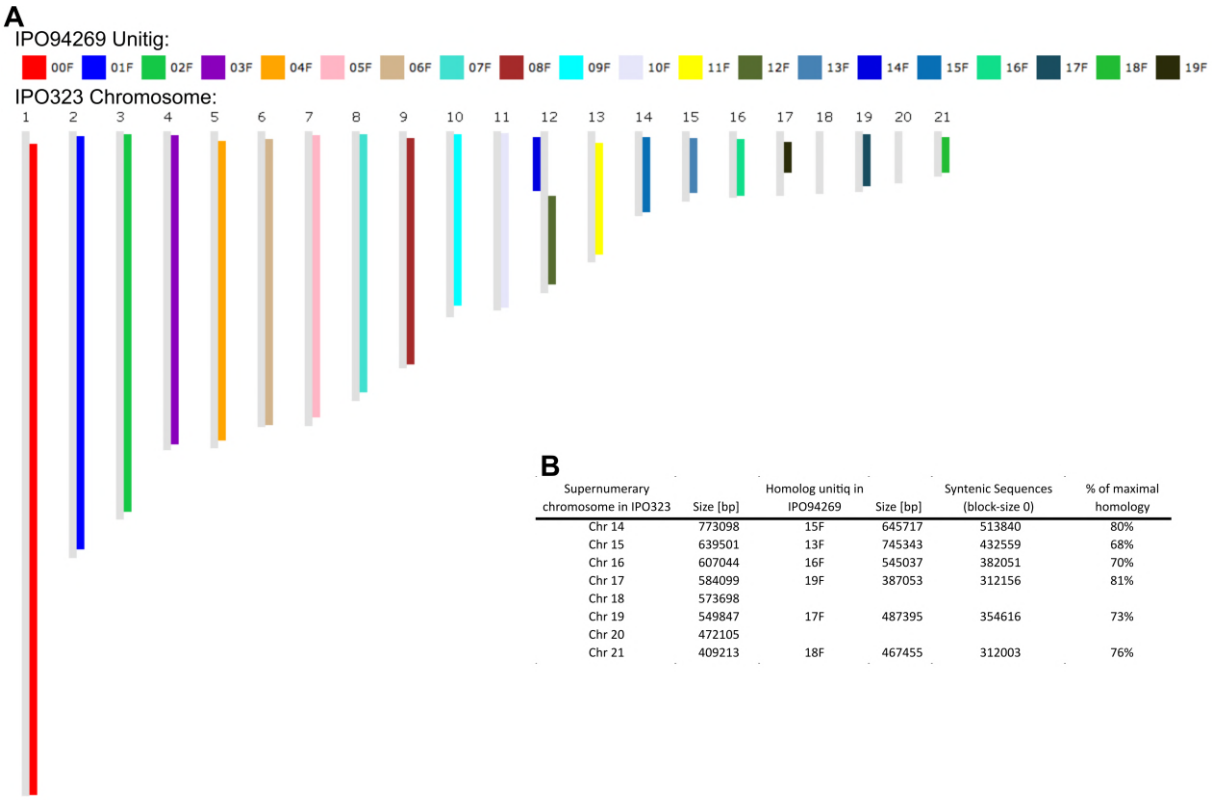

B

Supernumerary chromosome in IPO323	Size [bp]	Homolog unitiq in IPO94269	Size [bp]	Syntenic Sequences (block-size 0)	% of maximal homology
Chr 14	773098	15F	645717	513840	80%
Chr 15	639501	13F	745343	432559	68%
Chr 16	607044	16F	545037	382051	70%
Chr 17	584099	19F	387053	312156	81%
Chr 18	573698				
Chr 19	549847	17F	487395	354616	73%
Chr 20	472105				
Chr 21	409213	18F	467455	312003	76%

Figure S1. Synteny comparison of IPO94269 and IPO323. (A) Synteny blot for IPO94269 unitigs on IPO323 chromosomes. (B) Summary table of syntenic regions of IPO323 and IPO94269.

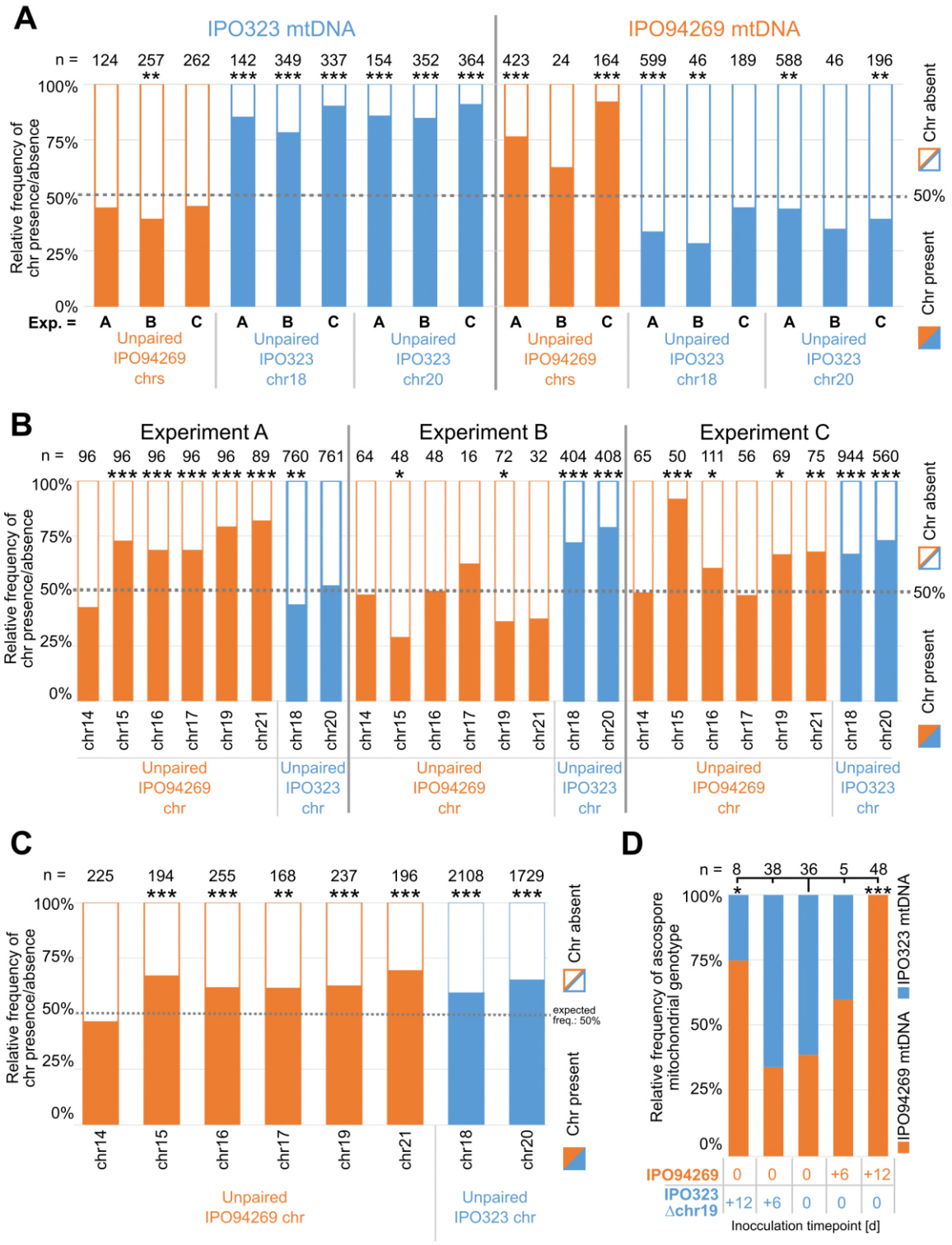

Figure S2. Transmission of unpaired chromosomes and mitochondria. (A) Detailed presence/absence frequencies for all unpaired supernumerary chromosomes according to the mitochondrial genotype present in all ascospores. Data for the three experiments A, B and C are depicted separately. Statistical significance was inferred by a two-sided binomial test with a probability of p=0.5. (B) Detailed presence/absence frequencies for all unpaired supernumerary chromosome in experiment A, B and C, restricted to all co-inoculation crosses using $1*10^7$ cells/mL cell density for both parental strains. Experiment A, B and C

differ in the observed transmission advantage for the chromosomes originating from the parent IPO94269 (orange) or IPO323 (blue). Statistical significance was inferred by a two-sided binomial test with a probability of p=0.5. (C) Presence/absence frequencies of all unpaired supernumerary chromosomes pooled for all three experiments A, B and C, restricted to all co-inoculation crosses using the $1*10^7$ cells/mL cell density for both parental strains. All supernumerary chromosomes, with the exception of chromosome 14 show a highly significant transmission advantage. Statistical significance was inferred by a two-sided binomial test with a probability of p=0.5. (D) Varying the infection time points impact the sexual role in crosses. Relative frequency of ascospore mitochondrial genotype is affected by the relative timing of the infection of the two parental strains IPO94269 (orange) and IPO323Δchr19. IPO94269 and IPO323Δchr19 were inoculated at either day 0, day +6 and day +12 creating situations were one parental strains had already established an infection when at day +6 and day +12 the other parental strains was inoculated on the same leaf. Parental strains infecting relatively later will preferentially assume the female role. Statistical significance was inferred by a two-sided Fisher's exact test compared to the co-inoculation of both strains at day 0. (* = p<0.05, ** = p<0.005, *** = p<0.0005, see Table S5 for details on all statistical tests).

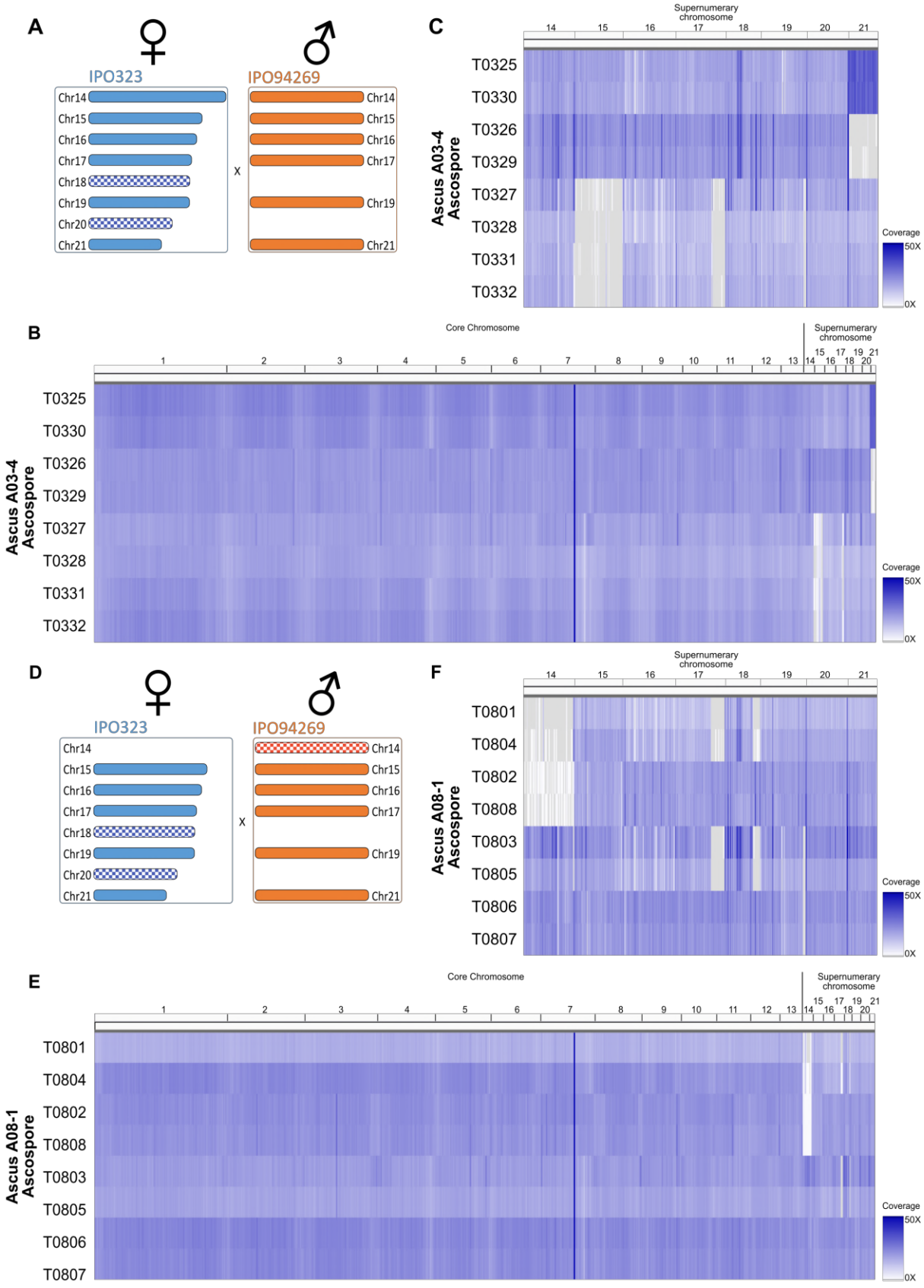

Figure S3. Whole genome sequencing confirms chromosome drive for unpaired supernumerary chromosomes. Coverage heatmap for eight ascospores (T0325-T0332) of ascus A03-4 (A-C) and eight ascospores (T0801-T0808) of ascus A08-1 (D-F). a)

Supernumerary chromosome complement in cross resulting in ascus A03-4 between IPO323 and IPO94269. (B) Heatmap coverage of all chromosomes on from ascus A03-4 reflecting similar coverage for essential and supernumerary chromosomes. (C) Heatmap coverage of supernumerary chromosomes of ascus A03-4 indicating constant coverage of chromosome 18 and 20 in all eight ascospores, loss of paired chromosome 15 in four ascospores and non-disjunction of sister-chromatids in meiosis 2 resulting in two ascospores containing two chromosomes 21 and two corresponding ascospores lacking chromosome 21. (D) Supernumerary chromosome complement in cross resulting in ascus A08-1 between PO323Δchr14 and IPO94269. (E) Heatmap coverage of all chromosomes on from ascus A08-1 reflecting similar coverage for essential and supernumerary chromosomes. (F) Heatmap coverage of supernumerary chromosomes of ascus A08-1 indicating constant coverage of chromosome 20 in all eight ascospores, segregating unpaired chromosome 14 inherited from the male parental strain and segregating loss of coverage on right arm of chromosome 18 in four ascospores.

Figure S4. Examples of gel-electrophoresis of PCR products for A) segregating marker of the mitochondrial genotype, B) segregating marker of the supernumerary chromosome 14, C) segregating marker of the supernumerary chromosome 15, D) segregating marker of the supernumerary chromosome 16, E) segregating marker of the supernumerary chromosome 17, F) segregating marker of the supernumerary chromosome 19, G) segregating marker of the supernumerary chromosome 19, H) subtelomeric marker of the supernumerary chromosome 19, I) subtelomeric marker of the supernumerary chromosome 19, J) segregating marker of the supernumerary chromosome 21, K) subtelomeric marker of the supernumerary chromosome 18, L) centromeric marker of the supernumerary chromosome 18, M) subtelomeric marker of the supernumerary chromosome 18, N) subtelomeric marker of the supernumerary chromosome 20, O) centromeric marker of the supernumerary chromosome 20, P) subtelomeric marker of the supernumerary chromosome 20.

(See attached PDF file)

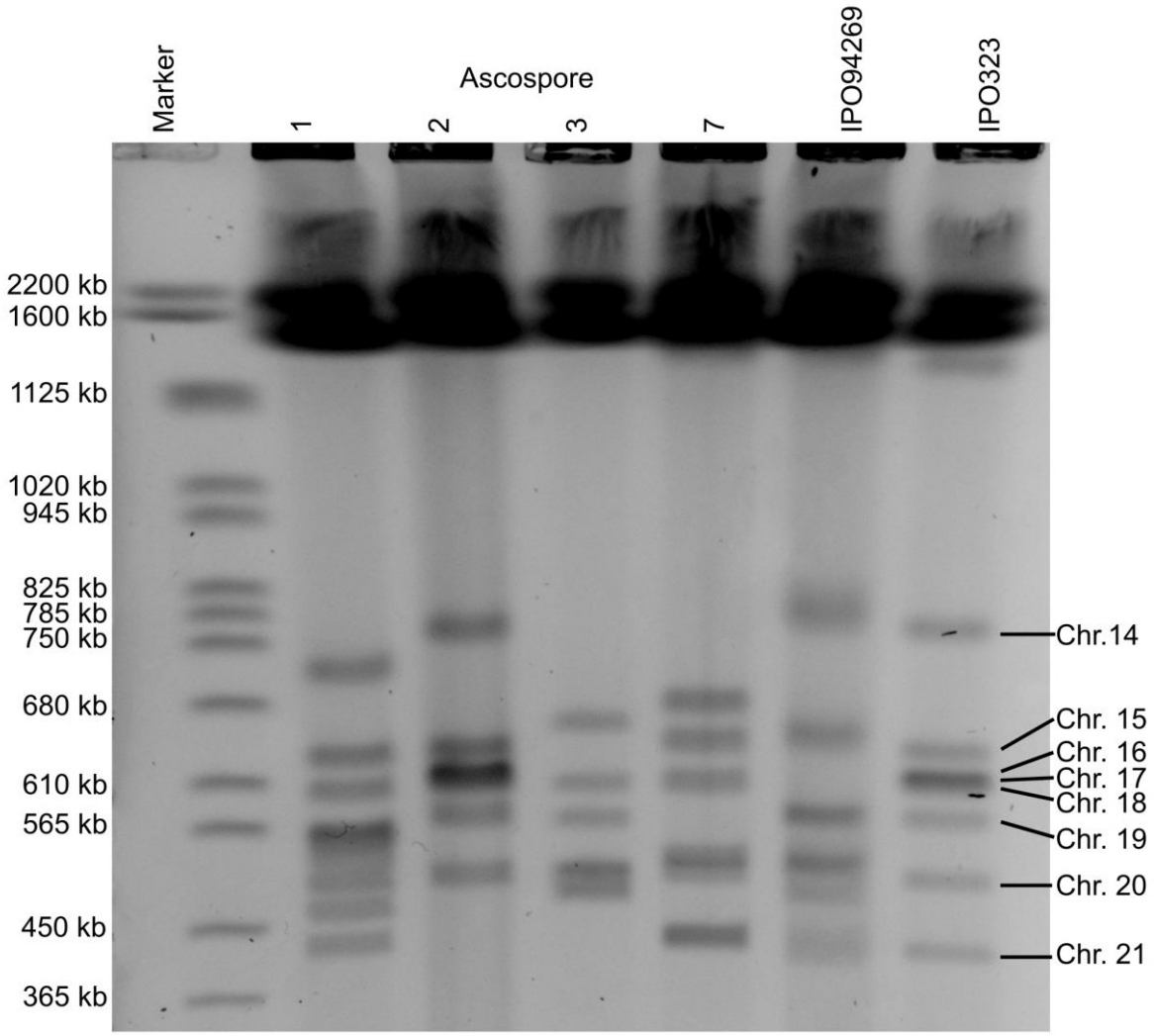

Figure S5. Pulsed-field gel electrophoresis (PFGE) of one unique ascospore per twin of the ascus A03-04, including the parental strains IPO94269 and IPO323. Although the parent IPO94269 does not contain chromosome 18 and 20, all progeny show a band of the expected sizes of chromosomes 18 and 20. Size marker: *Saccharomyces cerevisiae* chromosomes.

Supplementary Tables

Table S1. All primers used in this study.

Pimer Number	Full Primer Name	Sequence
879	oES879	CCGAGAAGGACCCAGCAAAC
880	oES880	TGACGGGAATGTCGGAGGTG
2100	chr_18	GTTTTCTCCCTGCACCTTGC
2101	chr_18	TATGGCACCTCCGAACAATG
2102	chr_18	GAGAATGTGGTCGCGGAGAT
2103	chr_18	GAGCCCTTCACCAACACACA
2108	chr_20	CGGTTCAGATCAGGTGCAAA
2109	chr_20	CGTGGAAGAGCATCGACAAG
2110	chr_20	GGCACCAACTGCACATGATT
2111	chr_20	ACATGCGAGCTGGATCTGAA
2902	chr21_cen	TGCGAAGCTCAAAAGAAGCG
2903	chr21_cen	TTGGAAGTCCGGAAAGACCG
2904	chr20_cen	ATGATGTGTTTGTGCCACGC
2905	chr20_cen	TACTGGACTAGCAAACCGCC
2906	chr19_cen	CAGCGTCAACAATCTCAGCG
2907	chr19_cen	TCCGAACCACGGATGTCTTG
2908	chr18_cen	AACAGTCGGCTAGCTGTTCC
2909	chr18_cen	TCCAGACGCAACGCACTTTA
2912	chr17_cen	CTGTGCTCTGTCATGGTGGT
2913	chr17_cen	TGATCACTGGACTGCGCTAC
2914	chr16_cen	GAATCCGGCTAGGTAAGCGA
2915	chr16_cen	TCTCTCCGGTCCTACTGTCG
2916	chr15_cen	CGGTCTTCGCGAATGAGAGT
2917	chr15_cen	GCGGATTTCTGGACCTGAGT
2918	chr14_cen	TACTGTTTCGGAGTGCCTGC
2919	chr14_cen	CCTACGGTGGACGCTACAAT
2972	11O21F	TCCACCTCTCTGGGCTGATT
2973	11O21R	CATTTCCTGCTTCTGGAGGT
2980	04L20F	GCGAATTGTTGAGAAGTCCA
2981	04L20R	TCTCGAAGGATCAGCGACAT
2994	Mt-SSR-F	CTCAGTTCAAGTCTGAGTGC
2995	Mt-SSR-R	GACGCACGCATTTCCACTCTA
2996	SSR_Goodwin2007 ac-0001	CACCACACCGTCGTTCAAG
2997	SSR_Goodwin2007 ac-0001	CGTAAGTTGGTGGAGATGG
2998	SSR_Goodwin2007 ggc-0001	GATACCAAGGTGGCCAAGG
2999	SSR_Goodwin2007 ggc-0001	CACGTTGGGAGTGTCGAAG
3000	SSR_Goodwin2007 caa-0002	TCTGCAGAGATCCCGTTACC
3001	SSR_Goodwin2007 caa-0002	ATCCATCACATGACGCACAC
3006	Chr14_SSR1	GCACTAATTGTCGTGACCGC
3007	Chr14_SSR1	CTCGTCTAGAAAGCCAGCGT
3008	Chr15_SSR2	CAACATGGGCGGGACAAAAG
3009	Chr15_SSR2	TCAAGACCAAAGTCCTCCCG
3010	Chr16_SSR3	CGATCGAAACGTGAACGCAA
3011	Chr16_SSR3	CTGTCACTGGAGATCACGGG
3012	Chr17_SSR4	ATCAAACCTACGTCCCTCGC
3013	Chr17_SSR4	CGTCCTTTGCCTCGAACAGA
3014	Chr19_SSR5	ACGATCGTATGTGTCGGACG
3015	Chr19_SSR5	GGGAAGGTGGACTGCATCTC
3016	Chr21_SSR6	GCAAGACCTTTTTCCCTCGC
3017	Chr21_SSR6	CCACTAGCACCTGGGAGTTC
3024	Zt94269_F17_R	CTACATCGACAGACGGGAGC
3025	Zt94269_F17_R	TGTTGAGGTAACGGGACGTG
MAT1-1F	mating type locus 1	CCGCTTTCTGGCTTCTTCGCACTG
MAT1-1R	mating type locus 1	TGGACACCATGGTGAGAGAACCT
MAT1-2F	mating type locus 2	GGCGCCTCCGAAGCAACT
MAT1-2R	mating type locus 2	GATGCGGTTCTGGACTGGAG
3093	IPO94269_Chr16_TelR_716F	GGGGACCGATTCGACCATAC
3094	IPO94269_Chr16_TelR_716R	CGATCGGTCTGTACTCAGCC

Table S2. Summary of all PCR marker results for experiment A.

(see attached Excel file)

Table S3. Summary of all PCR marker results for experiment B.

(see attached Excel file)

Table S4. Summary of all PCR marker results for experiment C.

(see attached Excel file)

Table S5 Summary of statistical tests performed in this study.

(see attached Excel file)

Table S6. Frequency of transmission of paired chromosomes to progeny ascospores.

Experiment	Paired chromosome	Count of ascospores in which chromosome is absent	Count of ascospores in which chromosome is present	Relative frequency	Pearson's Chi-squared test
A	Chr14	34	726	4.5%	X-squared = 34.422, df = 5, p-value = 1.962e-06
	Chr15	26	734	3.4%	
	Chr16	6	754	0.8%	
	Chr17	33	727	4.3%	
	Chr19	14	746	1.8%	
	Chr21	40	723	5.2%	
	Total A	**153**	**4410**	**3.4%**	
B	Chr14	19	352	5.1%	X-squared = 49.548, df = 5, p-value = 1.715e-09
	Chr15	31	356	8.0%	
	Chr16	0	388	0.0%	
	Chr17	22	397	5.3%	
	Chr19	4	359	1.1%	
	Chr21	32	372	7.9%	
	Total B	**108**	**2224**	**4.6%**	
C	Chr14	17	524	3.1%	X-squared = 22.513, df = 5, p-value = 0.0004181
	Chr15	24	535	4.3%	
	Chr16	5	495	1.0%	
	Chr17	35	522	6.3%	
	Chr19	20	519	3.7%	
	Chr21	15	472	3.1%	
	Total C	**116**	**3067**	**3.6%**	
	Total (A+B+C)	**377**	**9701**	**3.7%**	